Ponderomotive Optical Lattice for Rydberg Atoms

S. K. Dutta, J. R. Guest, D. Feldbaum, A. Walz-Flannigan, and G. Raithel
Department of Physics, University of Michigan, Ann Arbor, Michigan 48109-1120
(Received 31 August 2000)

We propose to use the ponderomotive energy of Rydberg electrons in standing-wave light fields to form an optical lattice for Rydberg atoms. Application of the Born-Oppenheimer approximation shows that, with readily achievable experimental parameters, atoms in any Rydberg state can be trapped. Realization of this scheme would extend the benefits of atom trapping to highly excited atoms.

PACS numbers: 32.80.Pj, 32.80.Lg

Trapping cold neutral atoms in periodic potentials known as optical lattices has been an active area of research [1]. While atoms in an optical lattice share some of the properties of electrons in a solid state lattice, optical lattices provide the added benefit that all lattice parameters—depth, lattice constants, phases, etc.—can be arbitrarily chosen and, if needed, varied as a function of time. This flexibility has given rise to a wide range of applications in the fields of quantum state generation and control [2] and quantum computation [3]. Extending these optomechanical structures to Rydberg atoms would substantially increase their functionality due to the large number of Rydberg states and the potentially long decoherence times in these atoms. While the production of cold Rydberg atoms has been proposed [4] and recently achieved through the Rydberg excitation of cold ground state atoms [5], the ability to subsequently trap the Rydberg atoms remains elusive.

The trapping force in conventional optical lattices arises from spatial modulations of the light shift induced by multiple interfering laser beams with a frequency near a transition between the trapped atomic ground state and another bound excited state [1]. While optical transitions between Rydberg states do not exist, the fact that the electron in a Rydberg atom is nearly free suggests that a potential due to the ponderomotive shift may be effective. The ponderomotive shift is the time averaged kinetic energy of a free electron in an oscillating electric field. For a field of the form $\mathcal{E}\cos(\omega t)$, the ponderomotive (or quiver) energy is

$$E^{\mathrm{Q}} = \frac{e^2|\mathcal{E}|^2}{4m_e\omega^2}, \tag{1}$$

where $-e$ and m_e are the electron charge and mass, respectively. For standing-wave optical fields, i.e., fields with a spatially periodic $\mathcal{E}(\mathbf{r})$, Eq. (1) represents a periodic potential from which free electrons can be diffracted (Kapitza-Dirac effect [6]). In this paper, we propose to use periodically modulated ponderomotive potentials to form *ponderomotive optical lattices* (POLs) for Rydberg atoms. We will show that these lattices are universal in that they can be used to trap atoms in any Rydberg state. In particular, we focus on circular Rydberg states ($l = n - 1$) because these states have maximal radiative lifetimes and their insensitivity to stray electric fields makes them ideal for high-precision spectroscopy and applications that require long quantum coherence times [7].

The motion of a Rydberg atom immersed in an optical field is described by the three coordinates $\boldsymbol{\rho}$, $\mathbf{r}$, and $\mathbf{R}$ (shown in Fig. 1) which are chosen such that they reflect the three time scales of the dynamics. The large separations between these time scales allow us to use the Born-Oppenheimer approximation (BOA). Since the separation in the time scales of the quiver motion (QM) and the motion in the other coordinates is the most explicit, we first adiabatically eliminate the QM. Thereafter, the relative motion (RM) of the electron around the ionic core (characterized by the coordinate $\mathbf{r}$) is adiabatically separated from the center-of-mass motion (CM). We thereby obtain a Schrödinger equation for the CM involving an adiabatic potential that is due to the driven electronic QM.

The $\boldsymbol{\rho}$ coordinate describes the QM of the Rydberg electron in the light field and has the fastest time scale (2.8×10^{14} Hz for 1064 nm light). The relative coordinate of the Rydberg electron, $\mathbf{r}$, evolves on various time scales as explained below. The fastest characteristic frequency of the RM is the Kepler frequency of the Rydberg electron, which for principal quantum numbers $n \sim 40$ is 10^{11} Hz. This leaves a comfortable factor of about 1000 to adiabatically separate the quiver and the orbital motion. Further, the amplitude of the QM of the electron is much smaller than the variation length of the atomic and external potentials. We can thus assume that the electron is quivering in a background potential $V_0(\mathbf{R} + \mathbf{r})$ that is constant

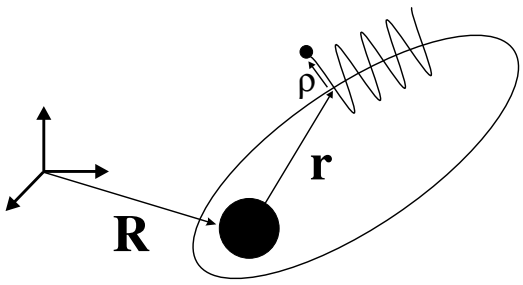

FIG. 1. The motion of a Rydberg atom in a laser field is characterized by a slowly evolving center-of-mass coordinate $\mathbf{R}$, a relative coordinate $\mathbf{r}$, and a quiver coordinate $\boldsymbol{\rho}$ evolving at the laser frequency.

on the fast time scale of the QM. The value of $V_0(\mathbf{R} + \mathbf{r})$ can be subtracted from the Schrödinger equation of the QM, yielding

$$\left\{-\frac{\hbar^2}{2m_e}\nabla_\rho^2 + e\boldsymbol{\rho}\cdot\mathcal{E}(\mathbf{R}+\mathbf{r})\cos(\omega t)\right\}\varphi(\boldsymbol{\rho},t;\mathbf{r},\mathbf{R}) = i\hbar\frac{\partial}{\partial t}\varphi(\boldsymbol{\rho},t;\mathbf{r},\mathbf{R}) \quad (2)$$

for the quiver wave function $\varphi(\boldsymbol{\rho},t;\mathbf{r},\mathbf{R})$, where $\mathbf{r}$ and $\mathbf{R}$ refer to the quasistatic parameters of the solution. The solutions of Eq. (2) are Volkov states [8], the energies of which are given by the ponderomotive potential

$$E^{\mathrm{Q}}(\mathbf{R}+\mathbf{r}) = \frac{e^2|\mathcal{E}(\mathbf{R}+\mathbf{r})|^2}{4m_e\omega^2}. \quad (3)$$

With the adiabatic elimination of the QM we can, from now on, account for the interaction between the Rydberg electron and the laser field by adding a static potential $E^{\mathrm{Q}}(\mathbf{R}+\mathbf{r})$ to the Hamiltonian of the Rydberg atom.

The typical Kepler frequency of Rydberg electrons is of order 100 GHz, while the expected order of magnitude of the CM oscillation frequency is 10 kHz. Therefore, at first glance it would appear that the RM has a much faster time scale than the CM and that, because of this, the adiabatic separation of the RM and CM would be straightforward. However, this impression is incorrect, as the RM can exhibit slow precession frequencies as described in the following. The high-angular-momentum states, which are of primary interest for Rydberg atom trapping, are embedded in $\approx n^2$-fold-degenerate manifolds of hydrogenic states [9]. Any external perturbation due to electric and magnetic fields mixes the hydrogenic states, thereby creating energy level splittings. According to the correspondence principle, the level splittings divided by h equal the precession frequencies of classical Rydberg electron orbits that are caused by the perturbing external fields. These precession frequencies represent the subtle slow time scales of the RM. To decide whether the BOA can be used in order to adiabatically separate the RM and the CM, all time scales of the RM—the Kepler period and the precession periods—need to be considered.

Static electric and magnetic fields $\mathbf{F}$ and $\mathbf{B}$ cause Stark and Zeeman splittings $3ea_0nF/2$ and $\mu_B B$, respectively (a_0 is the Bohr radius and μ_B the Bohr magneton) [9]. Even in weak stray electric fields—about 1 mV/cm—the Stark splitting divided by h is of the same order as the CM oscillation frequency (10 kHz). Thus, it appears difficult to make the BOA by having the precession frequencies much smaller than the CM oscillation frequency. Instead, one can make the precession frequencies much larger than the CM oscillation frequency by applying sufficiently large $\mathbf{F}$ and $\mathbf{B}$ fields. In the following, we first give a general account of this strategy, and then concentrate on an easy-to-solve example.

We assume that external static fields have been applied such that the BOA is valid, i.e., that the CM and the RM *are* adiabatically separable. If the BOA applies, the CM coordinate $\mathbf{R}$ can be considered a quasistatic parameter of the RM, yielding a RM Schrödinger equation

$$\{H_{\mathrm{F}} + E^{\mathrm{Q}}(\mathbf{R}+\mathbf{r})\}\psi(\mathbf{r};\mathbf{R}) = E^{\mathrm{R}}(\mathbf{R})\psi(\mathbf{r};\mathbf{R}), \quad (4)$$

where H_{F} is the sum of the atomic Hamiltonian and the static-field-induced perturbations of the RM and $\psi(\mathbf{r};\mathbf{R})$ is the wave function for the RM. For the BOA to be valid, it is sufficient that the spectrum of H_{F} is nondegenerate and all its level splittings are larger than the ponderomotive term in Eq. (4). If this is not the case, the BOA and the subsequent discussion in this paper may not apply. Fortunately, it is quite straightforward to find static fields for which H_{F} fulfills the mentioned conditions.

The solution of Eq. (4) yields energies $E_j^{\mathrm{R}}(\mathbf{R})$ and corresponding eigenstates of the RM coordinate, $\psi_j(\mathbf{r};\mathbf{R})$ (j is a state index). The dependence of the $E_j^{\mathrm{R}}(\mathbf{R})$ and the $\psi_j(\mathbf{r};\mathbf{R})$ on the CM-coordinate $\mathbf{R}$ is, in general, a result of the spatial variations of both the static fields $\mathbf{F}$ and $\mathbf{B}$ and the ponderomotive potential Eq. (3). The $E_j^{\mathrm{R}}(\mathbf{R})$ constitute *adiabatic potential surfaces* that govern the dynamics of the CM coordinate $\mathbf{R}$ which follows

$$\left\{-\frac{\hbar^2}{2M}\nabla_{\mathbf{R}}^2 + E_j^{\mathrm{R}}(\mathbf{R})\right\}\Phi_j(\mathbf{R}) = E_j^{\mathrm{C}}\Phi_j(\mathbf{R}). \quad (5)$$

E_j^{C} is the energy of the CM motion and $\Phi_j(\mathbf{R})$ is the CM wave function for Rydberg atoms in the RM state j. These atoms can be trapped in the POL if the wells of the periodic potential $E_j^{\mathrm{R}}(\mathbf{R})$ are deep enough to support localized states.

To find $E_j^{\mathrm{R}}(\mathbf{R})$, we solve Eq. (4) using nondegenerate first-order perturbation theory. The unperturbed Rydberg wave functions $\psi_j^0(\mathbf{r};\mathbf{R})$ and their energies $E_j^{\mathrm{R}0}(\mathbf{R})$ are defined by $H_{\mathrm{F}}\psi_j^0(\mathbf{r};\mathbf{R}) = E_j^{\mathrm{R}0}(\mathbf{R})\psi_j^0(\mathbf{r};\mathbf{R})$. The perturbed energies $E_j^{\mathrm{R}}(\mathbf{R})$ are then obtained as

$$E_j^{\mathrm{R}}(\mathbf{R}) = E_j^{\mathrm{R}0}(\mathbf{R}) + \frac{e^2}{4m_e\omega^2}\int d^3r|\mathcal{E}(\mathbf{R}+\mathbf{r})|^2|\psi_j^0(\mathbf{r};\mathbf{R})|^2. \quad (6)$$

A particularly transparent situation arises if H_{F} does not depend on $\mathbf{R}$, i.e., if the static fields applied to the atoms are homogeneous. Then, the Rydberg wave functions $\psi_j^0(\mathbf{r})$ and their energies $E_j^{\mathrm{R}0}$ to be used in Eq. (6) are the $\mathbf{R}$-independent eigenenergies and eigenfunctions of $H_{\mathrm{F}} = H_0 + e\mathbf{F}\cdot\mathbf{r} + \mu_B\mathbf{B}\cdot\mathbf{L}/\hbar$, where H_0 is the unperturbed atomic Hamiltonian (the diamagnetic energy is neglected). As one such example, we consider aligned circular Rydberg states $|n, l = n-1, |m| = n-1\rangle$ in a one-dimensional standing wave formed by two parallel linearly polarized, 3 mm diameter laser beams produced by a cw YAG laser (wavelength 1064 nm) with single-beam intensities 200 W/cm^2 and a mutual propagation angle 2α.

Parallel electric and magnetic fields **F** and **B** are used to lift the degeneracies of the hydrogenic Rydberg states to enforce the validity of the BOA. The direction of the fields **F** and **B** serves as the quantization axis for the internal atomic state and forms an angle θ with respect to the normal of the planes of the one-dimensional (1D) POL. The lattice normal is defined as the z axis. In parallel electric and magnetic fields, the circular-state wave functions are eigenfunctions of H_F. The degeneracy of the hydrogenic states is lifted as shown in Fig. 2 for the case $n = 40$. Since the linear Stark shift is $3ea_0nkF/2$ ($k = n_1 - n_2$, where n_1 and n_2 denote the parabolic quantum numbers [9]), the linear Stark effect does not entirely lift the degeneracies of the hydrogenic states, but splits them into degenerate submanifolds of states with the same k. The circular state, which has $n_1 = n_2 = 0$, is an element of the unshifted Stark submanifold, which contains all Rydberg states with $n_1 = n_2$ [9]. Since those states differ in the magnetic quantum number m, the residual degeneracies can be lifted by a weak magnetic field parallel to the electric field. At the expense of larger overall Stark shifts, the m degeneracy could also be lifted using the second-order Stark effect [9]. To calculate the POL trapping potential $E_j^R(z)$, we insert the wave function of the circular states into Eq. (6).

Figure 3a shows the effective potential $E_j^R(z)$ of circular Rydberg atoms for different principal quantum numbers n for $\theta = \pi/2$ and $\alpha = \pi/2$. The potential depth of $h \times 20$ kHz found for low n is equivalent to a temperature of 2 μK, which roughly equals the lower limit of laser cooling of Rb and Cs in optical molasses. For Rydberg wave functions that do not overlap with a significant fraction of the period of the POL, the **r** in the argument of $\mathcal{E}$ in Eq. (6) can be dropped. The potential of the POL then becomes identical to Eq. (1); i.e., it becomes independent of the Rydberg state $\psi_j^0(\mathbf{r})$ and simply mimics the light intensity distribution of the POL. In Fig. 3, this is the case for $n < 150$ and $n < 40$ for $\theta = 0$ and $\theta = \pi/2$, respectively. As n is increased, the size of the Rydberg wave function becomes of the order of the lattice constant, and the ponderomotive potential becomes partially washed out due to the averaging specified by Eq. (6). If the spatial extent of the Rydberg atom in the direction of the lattice normal is of the order of an odd integer times the lattice constant, the POL potential is reversed, as the CM coordinate is attracted to *maxima* of $|\mathcal{E}|^2$ of the optical standing wave (hatched ranges in Fig. 3). A free electron, in contrast, would be attracted to the minima of $|\mathcal{E}|^2$.

The anticipated application of POLs as traps that suspend Rydberg atoms against gravity while they are spectroscopically analyzed or manipulated entails several considerations. For reasonable laser intensities, the *maximum acceleration* should be $\gg g$ (for earth-bound experiments). To minimize the sensitivity of the trapped atoms to common environmental vibrations of the lattice, the *CM oscillation frequency* should be at least a few kHz. A large CM frequency will also facilitate a spectroscopic resolution of the CM energy quantization in the POL. The RM energy difference ΔE between two Rydberg states A and B of the above Hamiltonian H_F can, in principle, be accurately determined by preparing the atoms in the CM ground state of A and measuring the transition frequency ν to the CM ground state of B. Then, $\Delta E = h\nu + E_{g,A}^C - E_{g,B}^C$, where $E_{g,A}^C - E_{g,B}^C$, the difference between the CM ground state energies of A and B, represents a *trap-induced shift*. The trap-induced shift must be minimized in order to minimize the measurement error of ΔE. Further, the well-to-well *tunneling rates* of the CM ground states should be smaller than the natural decay rate. These parameters can be efficiently controlled using the lattice geometry, as shown in Fig. 4 for the case of $n = 40$ circular rubidium Rydberg atoms in a 1D POL with $\theta = \pi/2$ and α varying from zero to $\pi/2$. In the given example, a favorable compromise between a large POL trapping force and a CM quantization structure suitable for high-precision spectroscopy is achieved for angles $\alpha \approx \pi/4$.

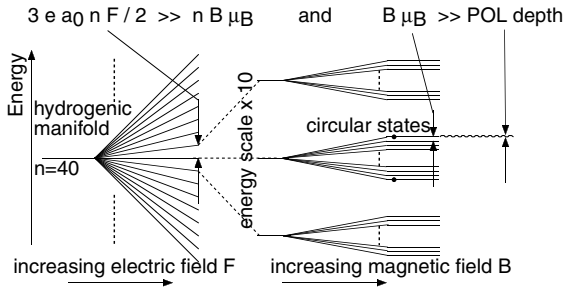

FIG. 2. Splitting scheme used to isolate $n = 40$ circular Rydberg states and trap them in ponderomotive optical lattices. An electric field of 0.1 V/cm separates the hydrogenic manifold into submanifolds with a splitting of order 10 MHz. A parallel magnetic field of order 0.1 G removes the residual degeneracies. A standing light wave spatially modulates the circular-state energy with a modulation depth of about 10 kHz, creating microscopic potential traps for the Rydberg atoms.

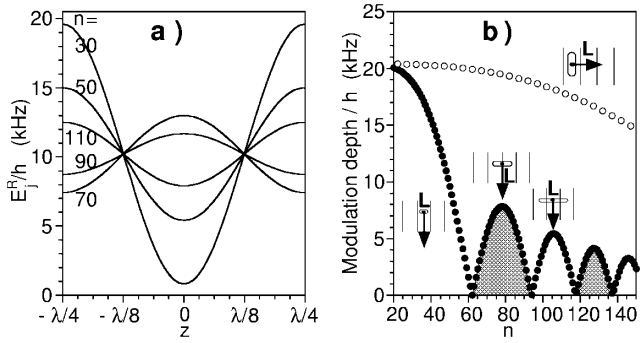

FIG. 3. Trapping potential $E_j^R(z)$ created by the 1D-POL discussed in the text. (a) Potential vs position for circular states with the indicated values of n and $\theta = \pi/2$. (b) Modulation depth for circular states with $\theta = \pi/2$ (filled dots) and $\theta = 0$ (open dots). The lattice is reversed in the hatched ranges of n. The insets indicate the orientation and spatial extent of the Rydberg atoms in the lattice, where **L** denotes their angular momentum vector and the thin lines represent the maxima of $|\mathcal{E}|^2$.

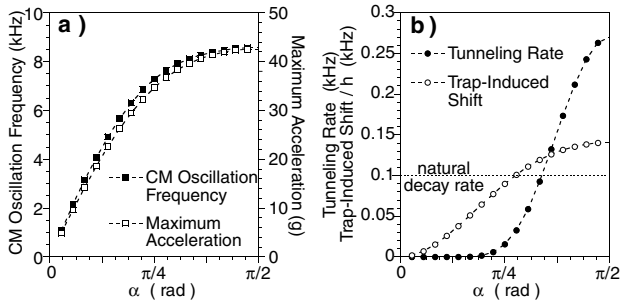

FIG. 4. CM oscillation frequency (filled squares), maximum acceleration (open squares), and the tunneling rate (filled dots) for $n = 40$ circular Rydberg atoms vs the beam angle α for the POL explained in the text. We also show the trap-induced frequency shift of the transition between $n = 40$ and $n = 39$ circular states trapped in the CM ground states of the POL (open dots). In a spectroscopic experiment, the tunneling rate and the trap-induced shift/h should not exceed the natural decay rate (dotted line) of the involved Rydberg levels.

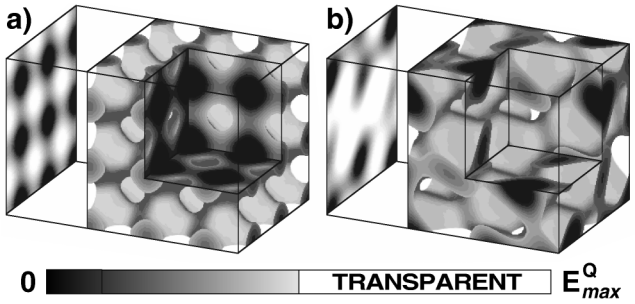

FIG. 5. Three-dimensional plots of ponderomotive potentials $E^{Q}(\mathbf{R})$ spanning a 2 μm cube. (a) Six-beam 3D cubic lattice. (b) Six-beam 3D skewed lattice.

The ponderomotive shift is not sensitive to the temporal phases between the linear polarization components; at a given location $\mathbf{s}$ it is $\propto|\mathcal{E}_x(\mathbf{s})|^2 + |\mathcal{E}_y(\mathbf{s})|^2 + |\mathcal{E}_z(\mathbf{s})|^2$. Thus, a three-dimensional (3D) cubic POL can be formed using three pairs of laser beams with mutually orthogonal linear polarizations, without the need for stabilizing the relative phases between the beams. An example of a 3D cubic POL is shown in Fig. 5a. The 3D lattice does not need to be orthogonal; in Fig. 5b an example of a skewed lattice is shown.

In the following, we compare POLs with conventional optical lattices [1]. The internal motion of Rydberg atoms spans a Hilbert space much larger than that of atoms in low-lying states. Despite this, the separation of the internal and CM dynamics based on the BOA is similar in POLs and conventional optical lattices [10]. Because of the $|\mathcal{E}|^2$ dependence of the ponderomotive shift, POLs can be produced only by intensity gradients, not by polarization gradients. Further, in POLs the physical size of the trapped atoms can be comparable to the lattice constant, whereas atoms in conventional lattices appear as point objects on the length scale of the lattice. In POLs, some trapped atoms may be lost due to photoionization. These losses will be negligible; we estimate that in a POL formed by two counterpropagating YAG beams ($\lambda = 1064$ nm) with 200 W/cm^2 intensity low-l Rydberg states ionize with $<1\%$ probability per natural lifetime. For long-lived high-l Rydberg states we have found photoionization probabilities $<10^{-5}$ (estimates are for $n > 30$).

In the future, POLs may be used to localize Rydberg atoms in space, to suppress their collisions and to store them for long periods of time. Microwave spectroscopy on such well-prepared samples of Rydberg atoms may lead to improved determinations of atomic parameters and the Rydberg constant. Modulations of the POL can also be used to coherently couple Rydberg states. Driven transitions between Rydberg states of atoms trapped in POLs can be made lattice-site-selective using quasistatic electric and magnetic gradient fields that cause position-dependent shifts of the transition frequency. Such tools may lead to novel approaches in quantum information and computation. A POL densely occupied with circular Rydberg atoms may display a Mott transition, thus forming a novel metastable, dilute, light-stabilized, metallic form of matter. These are only a few examples how future research can benefit from ponderomotive optical lattices for Rydberg atoms.

We acknowledge support by the NSF (Grant No. PHY-9875553) and by the Chemical Sciences, Geosciences and Biosciences Division of the Office of Basic Energy Sciences, Office of Science, U.S. Department of Energy.

[1] P. S. Jessen and I. H. Deutsch, Adv. At. Mol. Opt. Phys. **37**, 95 (1996); D. R. Meacher, Contemp. Phys. **39**, 329 (1998).
[2] G. Raithel, W. D. Phillips, and S. L. Rolston, Phys. Rev. Lett. **81**, 3615 (1998), and references therein.
[3] G. K. Brennen, C. M. Caves, P. S. Jessen, and I. H. Deutsch, Phys. Rev. Lett. **82**, 1060 (1999).
[4] J. Guo and E. Arimondo, Phys. Rev. A **53**, R1224 (1996).
[5] W. R. Anderson, J. R. Veale, and T. F. Gallagher, Phys. Rev. Lett. **80**, 249 (1998); I. Mourachko *et al.,* Phys. Rev. Lett. **80**, 253 (1998); T. C. Killian *et al.,* Phys. Rev. Lett. **83**, 4776 (1999); S. Dutta, D. Feldbaum, and G. Raithel, LANL e-print http://xxx.lanl.gov/abs/physics/0003109, 2000.
[6] P. H. Bucksbaum, D. W. Schumacher, and M. Bashkansky, Phys. Rev. Lett. **61**, 1182 (1988).
[7] R. Lutwak, J. Holley, P. P. Chang, S. Paine, D. Kleppner, and T. Ducas, Phys. Rev. A **56**, 1443 (1997).
[8] H. Friedrich, *Theoretical Atomic Physics* (Springer, Berlin, 1998).
[9] T. F. Gallagher, *Rydberg Atoms* (Cambridge University Press, Cambridge, 1994).
[10] S. K. Dutta and G. Raithel, J. Opt. B Quantum Semiclass. Opt. **2**, 651 (2000).